



A model-based approach to the Common-Diffraction-Surface Stack method – a synthetic case study

Hashem Shahsavani¹, Jürgen Mann², Iradj Piruz¹, and Peter Hubral²

¹ Faculty of Mining, Petroleum and Geophysics, Shahrood University of Technology, Shahrood, Iran

² Geophysical Institute, Karlsruhe Institute of Technology, Hertzstraße 16, 76187 Karlsruhe, Germany

Copyright 2011, SBGf - Sociedade Brasileira de Geofísica.

This paper was prepared for presentation at the Twelfth International Congress of the Brazilian Geophysical Society, held in Rio de Janeiro, Brazil, August 15-18, 2011.

Contents of this paper were reviewed by the Technical Committee of the Twelfth International Congress of The Brazilian Geophysical Society and do not necessarily represent any position of the SBGf, its officers or members. Electronic reproduction or storage of any part of this paper for commercial purposes without the written consent of The Brazilian Geophysical Society is prohibited.

Abstract

The Common-Reflection-Surface (CRS) stack method parameterizes and stacks seismic reflection events in a generalized stacking velocity analysis. It considers a discrete number of events contributing to a given stack sample such that conflicting dip situations can be handled. The reliable detection of such situations is difficult and missed contributions to the stacked section cause artifacts in a subsequent poststack migration. This is deleterious for complex data where prestack migration is no viable option due to its demands on velocity model accuracy, such that we might have to rely on poststack migration. As an alternative, the conflicting dip problem has been addressed by explicitly considering a virtually continuous range of dips with a simplified stacking operator in a process termed Common-Diffraction-Surface (CDS) stack. In analogy to the CRS stack, the CDS stack has been implemented and successfully applied in a data-driven manner based on coherence analysis in the prestack data. In view of the computational costs, we present a more efficient model-based approach to the CDS stack designed to generate stack sections optimized to image discontinuities by poststack migration. This approach only requires a smooth macro-velocity model of minor accuracy. We present our results for the synthetic Sigsbee 2A data and compare them to the results of CRS stack and data-driven CDS stack.

Introduction

The CRS stack method follows the concept of the classical stacking velocity analysis, the local parameterization and stacking of reflection events by means of an analytic second-order approximation of the reflection traveltimes (see, e.g., Müller, 1998; Mann et al., 1999; Jäger et al., 2001). In its simplest implementation, the CRS stack determines only one optimum stacking operator for each zero-offset (ZO) sample to be simulated. Along this operator, we obtain the maximum coherence in the seismic reflection data. However, in the presence of curved reflectors or diffractors, various events might intersect each other and/or themselves, such that a single stacking operator per ZO sample is no longer appropriate. Thus, Mann (2001) proposed to allow for a small, discrete number

of stacking operators for a particular ZO sample. The main difficulty in this approach is to identify conflicting dip situations and to decide how many contributions should be considered. This implies a tricky balancing between lacking contributions and potential artifacts due to the unwanted parameterization of spurious events.

Soleimani et al. (2009b,a) proposed an adapted CRS strategy designed to obtain a stacked section as complete as possible by merging concepts of the dip moveout correction with the CRS approach: instead of only a discrete number of dips, a virtually continuous range of dips is considered. To simplify this process and to emphasize diffraction events, this has been implemented with a CRS operator reduced to (hypothetical) diffraction events: this CDS stack approach has been successfully applied to complex land data (Soleimani et al., 2010). However, the approach is quite time consuming, as separate stacking operators have to be determined for each stacked sample to be simulated and each considered dip in a data-driven manner by means of coherence analysis in the prestack data.

Here, we propose an efficient model-based approach to the CDS stack. We assume that a smooth macro-velocity model has already been determined in which the parameters of the CDS stacking operators can be easily forward-modeled.

Traveltime approximation

The CRS method is based on an analytical approximation of the reflection traveltimes up to second order in terms of the half source/receiver offset h and the displacement of the source/receiver midpoint x_m with respect to the location x_0 of the stacked trace to be simulated. For the 2D case considered in this abstract, the hyperbolic CRS traveltimes approximation can be expressed as

$$t^2(x_m, h) = \left[t_0 + \frac{2 \sin \alpha}{v_0} (x_m - x_0) \right]^2 + \frac{2t_0 \cos^2 \alpha}{v_0} \left[\frac{(x_m - x_0)^2}{R_N} + \frac{h^2}{R_{NIP}} \right], \quad (1)$$

with v_0 denoting the near-surface velocity. The stacking parameter α is the emergence angle of the normal ray, whereas R_N and R_{NIP} are the local radii of hypothetical wavefronts excited by an exploding reflector experiment or an exploding point source at the (unknown) reflection point of the normal ray, the normal incidence point (NIP). All these properties are defined at the acquisition surface ($x_0, z = 0$).

For a true diffractor in the subsurface, an exploding point source experiment and an exploding reflector experiment naturally coincide such that $R_{\text{NIP}} \equiv R_{\text{N}}$. Thus, for *diffraction* events, the CRS traveltimes equation (1) reduces to the CDS traveltimes approximation

$$t^2(x_m, h) = \left[t_0 + \frac{2 \sin \alpha}{v_0} (x_m - x_0) \right]^2 + \frac{2t_0 \cos^2 \alpha}{v_0 R_{\text{CDS}}} \left[(x_m - x_0)^2 + h^2 \right], \quad (2)$$

with $R_{\text{CDS}} \equiv R_{\text{NIP}} \equiv R_{\text{N}}$. For *reflection* events, the CDS operator (2) is an inferior approximation compared to the full CRS operator (1) as $R_{\text{NIP}} \neq R_{\text{N}}$. Nevertheless, it still allows to approximate the event within a reasonably chosen aperture, see below. For the data-driven CDS stack, this simplified operator has been chosen for performance reasons. For the model-based CDS stack, this simplification is mandatory, as there is no structural information on reflector curvatures contained in the considered smooth macro-velocity model. Thus, a forward-modeling of the lacking parameter R_{N} is not possible anyway.

Forward-modeling

The radius of the NIP wave occurring in the CDS operator (2) is associated with a hypothetical point source at the NIP. The local curvature of the corresponding wavefront is considered along the normal ray. Thus, the first step is to determine the potential normal ray by means of kinematic ray tracing. As we need this ray for a given surface location and a given emergence angle, the kinematic ray tracing is performed for the down-going ray. Kinematic ray tracing consists in the calculation of the characteristics of the Eikonal equation. We have chosen the particular system for which the variable along the ray is directly the traveltimes, as we have to compute ray tracing results for a regular grid in ZO traveltimes. The corresponding kinematic ray tracing system, in 2D a system of four coupled ordinary differential equations of first order, can be numerically integrated with the well known Runge-Kutta scheme of fourth order.

The determination of R_{NIP} requires dynamic ray tracing along the ray path. The 2D dynamic ray tracing system consists of two coupled ordinary differential equations of first order. For a given initial condition at a point of the ray, it allows to calculate the second partial derivative of traveltimes normal to the ray for any point along the ray. For a point source initial condition at a NIP on the ray, this traveltimes derivative yields the searched-for stacking parameter. However, it is highly inefficient to integrate the dynamic ray tracing system upwards along the ray, as this had to be performed separately for each considered point on the ray, i. e., hundreds or thousands of times along each ray. Instead, it is far more efficient to perform the dynamic ray tracing in parallel to the kinematic ray tracing along the down-going ray twice, for two mutually orthogonal initial conditions: one corresponds to a point source, the other to a plane wave source at the emergence point of the ray. With the two orthogonal solutions along the ray, we can directly compute the solution for any arbitrary initial condition at any point of the ray, indeed also in its reverse direction. Thus, the searched-for solution for a point source at the NIP is readily available for all potential NIPs along the ray.

Stacking aperture

In the data-driven stack approaches, the size of the search and stacking aperture in midpoint direction is often based on the size of the (estimated) projected first Fresnel zone. Furthermore, the aperture size has to be kept constant for a particular ZO sample as coherence measures are sensitive to the number of contributing traces which might deteriorate the coherence analysis (see, e.g., Mann, 2002). In the model-based approach, coherence analysis is not employed, such that there is no need for a fixed aperture. In addition, the aperture size in midpoint direction has to be chosen smaller, as the CDS approximation with $R_{\text{CDS}} \equiv R_{\text{NIP}}$ quickly deviates from the actual event in case of a reflection event. Therefore, we propose to use a smaller aperture centered around the so-called Common-Reflection-Point (CRP) trajectory, where CRS operator and CDS operator are both tangent to the actual event. In a second order approximation, the projection of the CRP trajectory onto the acquisition surface reads (Höcht et al., 1999)

$$x_m(h) = x_0 + r_T \left(\sqrt{\frac{h^2}{r_T^2} + 1} - 1 \right) \quad \text{with} \quad r_T = \frac{R_{\text{NIP}}}{2 \sin \alpha}. \quad (3)$$

Obviously, all required properties are available from the dynamic ray tracing. Along the CRP trajectory, we can use comparatively small midpoint apertures and still ensure that we capture the contributions from the area of tangency between event and operator. The aperture width controls the balance between diffraction and reflections events.

Synthetic data example: Sigsbee 2A

To allow for a direct comparison with the data-driven CDS results by Soleimani et al. (2009a) we applied the model-based CDS approach to the well-known synthetic Sigsbee 2A data set (Pfaffenholz, 2001). This data set has been simulated by the SMAART JV by acoustic finite-difference modeling for the stratigraphic model shown in Figure 1. Due to an absorbing top surface, the data contain no free-surface multiples. They consist of a total of 500 shot gathers with 150 ft shot interval and up to 348 receivers with a spacing of 75 ft. Temporal sampling rate is 8 ms, offsets range from 0 to 26025 ft.

As we want to focus on the stacking procedure rather than on the generation of the macro-velocity model by means of an inversion, we used the migration velocity model (not shown) distributed with the data as basis for our macro-velocity model. The migration velocity model consists of the water column, the salt body, and a smooth background velocity, namely a constant vertical gradient of 0.3/s starting with 5000 ft/s at the seafloor. To obtain our macro-model, we first restored the seafloor at those locations where the salt body is in direct contact with the water column and then replaced the salt body by the background gradient. Finally, we smoothed the inverse of the velocity model to get rid of the sharp velocity contrast at the seafloor without impairing the kinematics of the model.

The kinematic and dynamic ray tracing has been performed for each CMP bin at a lateral spacing of 37.5 ft and a temporal step length of 0.8 ms. Rays have been shot for an angle range of $\pm 50^\circ$ at 2° spacing. For the stacking process, the stacking parameter R_{CDS} is linearly interpolated in between the rays on a grid with 1° spacing.

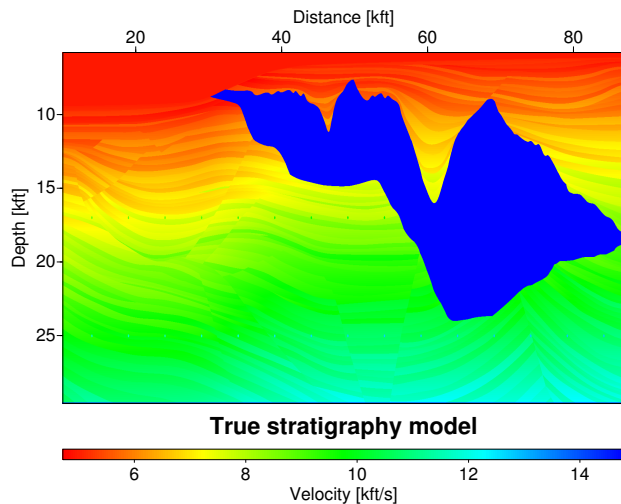


Figure 1: Stratigraphic model used for the simulation of the Sigsbee 2A data.

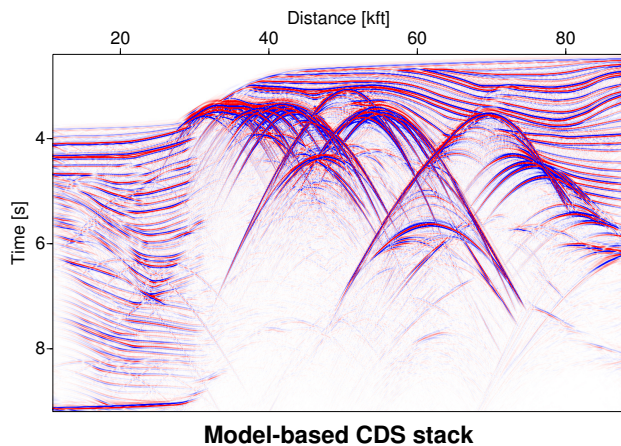


Figure 2: Stacked section obtained with the model-based CDS approach. Note the various diffraction patterns caused by true diffractors, wedges, and model discretization.

The midpoint aperture has a constant half-width of 300 ft centered around the approximate CRP trajectory (3), the offset aperture ranges from 6000 ft at 2.3 s to 25000 ft at 11 s ZO travelttime. Semblance has been calculated within a time window of 56 ms.

The stacked section shown in Figure 2 is quite similar to the corresponding result obtained with its data-driven counterpart by Soleimani et al. (2009a) (not shown). The main difference is the computational cost which is now more than two orders of magnitude lower for this data set (not including the fact that the data-driven result excludes the subsalt region for performance reasons). Of course, with the inherent second-order approximation of the CRS and CDS approaches, we cannot expect any reasonable result for the subsalt region, that is why we have removed the salt body in the macro-velocity model.

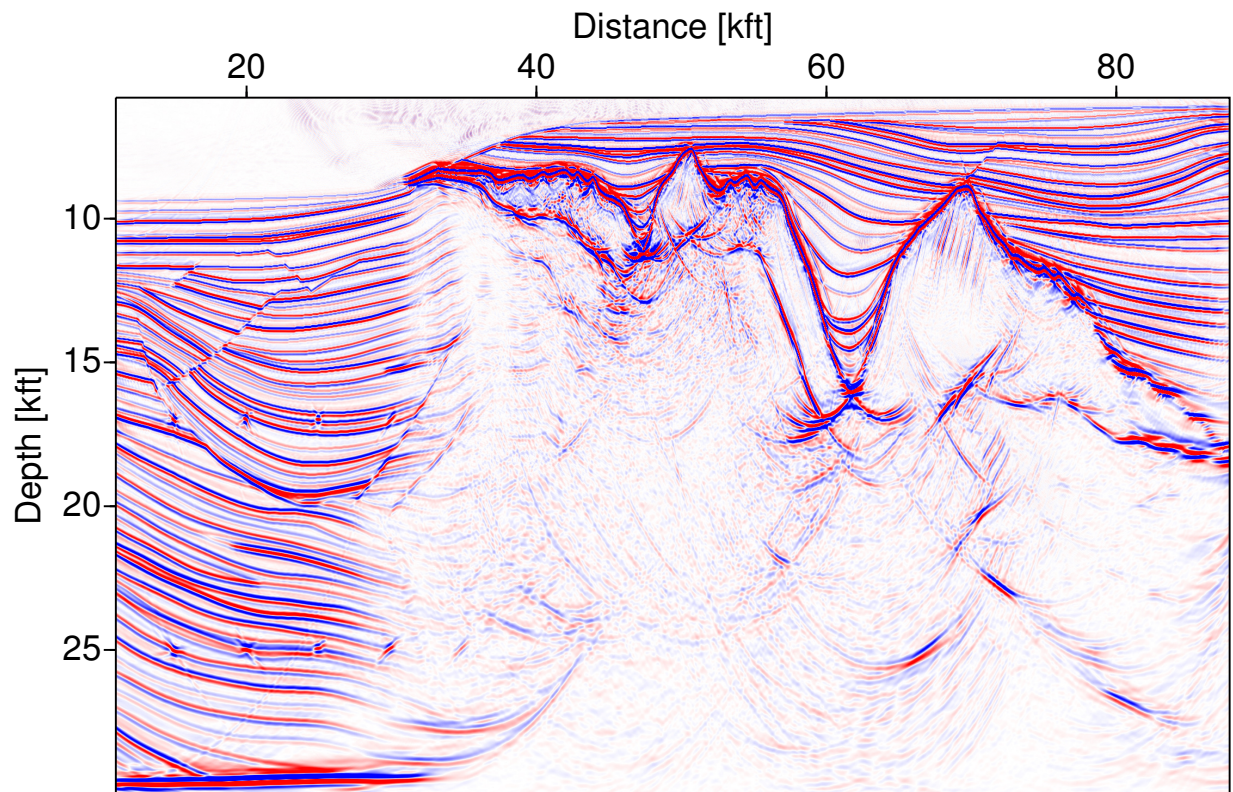
The benefits of the complete handling of conflicting dip situations are best seen after a subsequent poststack migration using the above described macro-velocity model

derived from the original migration velocity model. Figure 3 (top) shows the result of a poststack migration obtained for the model-based stack section shown in Figure 2. All faults and diffractors are well focused, everything left of and above the salt is well imaged.

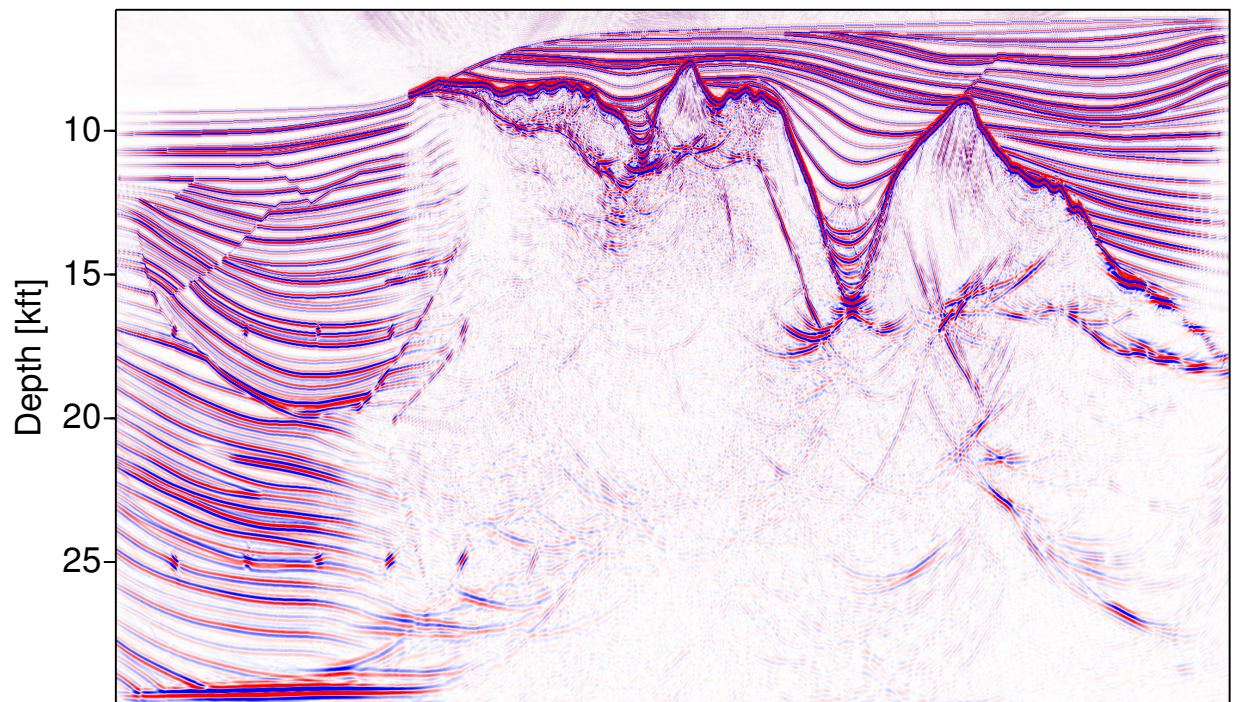
As a reference, we also applied a Kirchhoff prestack depth migration to the prestack data using the same macro-velocity model. The offset range and the muting of the migrated image gathers were chosen such that they match the corresponding parameters used during the CDS stack as closely as possible. Figure 3 (bottom) shows the stack of about 80 offset bins with a width of 300 ft each after depth-dependent muting. This section is very similar to the poststack migration of the model-based CDS-stacked section in Figure 2. Note that (of course, except for the subsalt part) the prestack migration has been performed with an optimum, i. e., kinematically perfectly correct velocity model. For less accurate models as usually achievable for real data, the prestack migration result will suffer much more from inaccuracy than the model-based CDS stack and the subsequent poststack migration.

For comparison, we first revisited the CRS results by Mann (2002). They have been computed with two strategies: the simple approach considering only one dip per ZO sample and the extended approach with up to three dipoles per ZO sample. The poststack migration of the latter is depicted in Figure 4 (bottom). Faults and diffractors are only partly focused. Spurious events in the stacked section, e.g. associated with a change of the number of contributions from sample to sample, cause various artifacts showing up as isochrones in the migrated section. The result based on the CRS stack with only one dip (not displayed) differs from the multi-dip CRS-stacked section in two respects: on the one hand, due to the lacking contributions at conflicting dip locations, the diffractors and faults appear even less focused and with lower amplitudes. On the other hand, the stacked section contains less spurious events such that we have less artifacts in the migrated section. In both cases, the results of poststack migration are unsatisfactory. The synclines in the top salt are incomplete and accompanied by coherent artifacts at slightly larger depths. As discussed by Mann (2002), the CRS stack has most likely also parameterized and stacked events associated with prismatic waves which lead to additional events in the stacked section. CRS for ZO simulation as well as poststack migration both imply normal rays, such that prismatic waves cannot be correctly imaged. Note that this effect hardly occurs in the model-based result shown in Figure 3 (top): As we explicitly forward-model normal rays there, the events from prismatic waves are attenuated by destructive interference.

For the next comparison, we revisited the data-driven CDS results by Soleimani et al. (2009a). The corresponding poststack-migrated section displayed in Figure 4 (top) shows well focused diffractors and faults and much less artifacts caused by spurious events compared to the CRS-based result in Figure 4 (bottom). As in the CRS-based result, the synclines in the top salt are still not properly imaged, as the data-driven CDS stack picks up prismatic waves as well. Note that the lower right part of the stacked section has not been computed for performance reasons such that this area remains either empty or shows some isochrones in the migrated section.

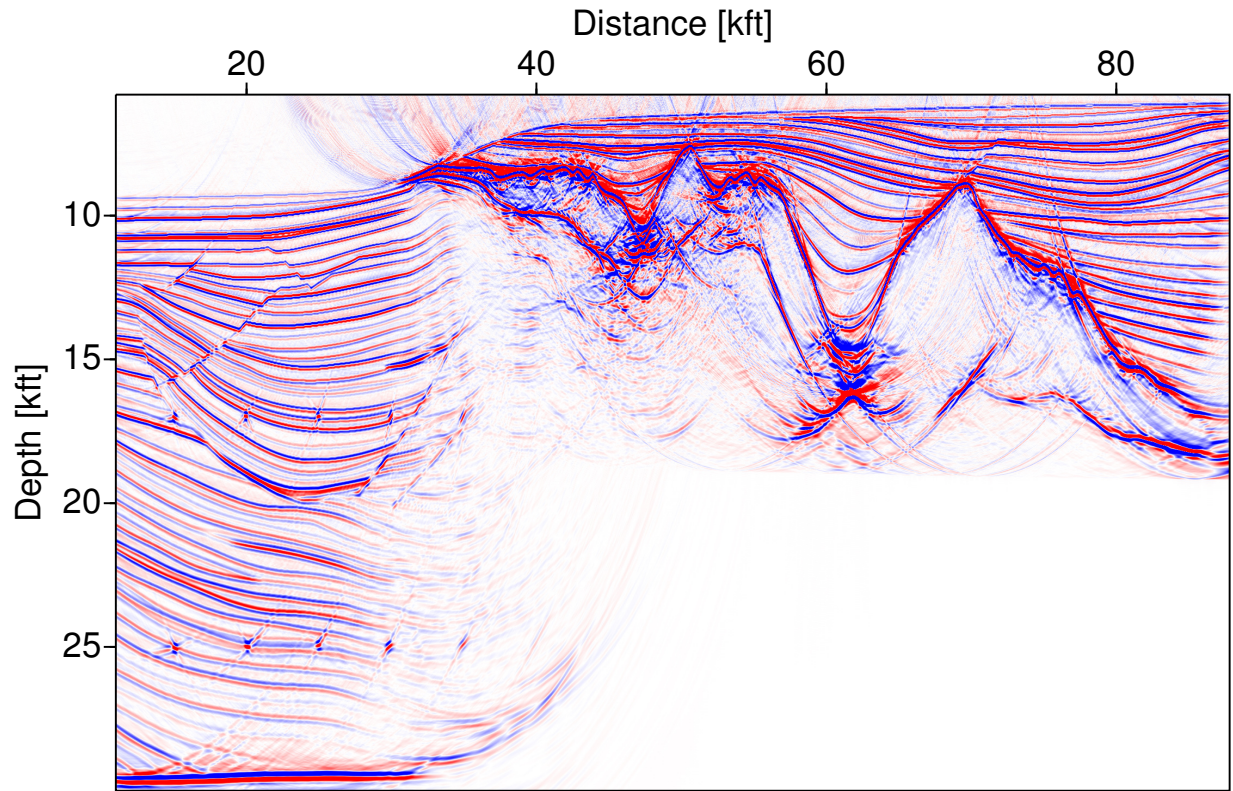


PostSDM of model-based CDS stack

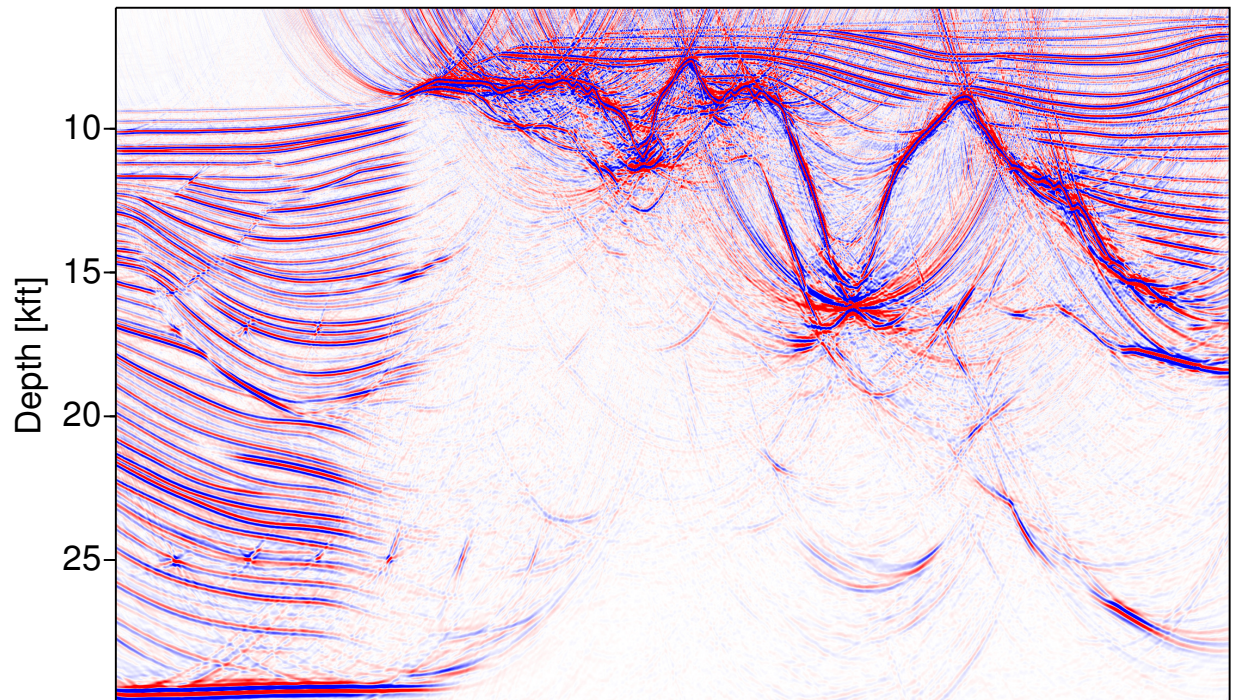


Prestack depth migration

Figure 3: Top: poststack Kirchhoff depth migration result for the model-based stack section shown in Figure 2. Faults and diffractors are clearly focused. Bottom: prestack Kirchhoff depth migration result with high similarity to the poststack result shown above. To allow for a fair comparison, the used offset range coincides with the one used for the CDS stack and the image gathers have been muted such that they mimic the time-dependent CDS stacking aperture in offset direction.



PostSDM of data-driven CDS stack



PostSDM of CRS stack

Figure 4: Top: poststack Kirchhoff depth migration result for the data-driven CDS result published by [Soleimani et al. \(2009a\)](#). Faults and diffractors are well focused, there are only few isochrones caused by spurious events. Bottom: poststack Kirchhoff depth migration result for the CRS stack result published by [Mann \(2002\)](#). Up to three dips have been considered for each ZO sample. Faults and diffractors are only partly focused, many isochrones caused by spurious events can be seen.

Conclusions and outlook

We have implemented and applied a model-based approach to the CDS stack method. This method is intended to fully resolve the conflicting dip problem occurring in complex data and, thus, to allow to simulate a complete stacked section containing all mutually interfering reflection and/or diffraction events. In contrast to the entirely data-driven CDS method, this model-based approach is far more efficient. The required macro-velocity model can be generated with any inversion method, including the sequential application of CRS stack and NIP-wave tomography. For the presented Sigsbee 2A data, we excluded the inversion aspect and used a simplified version of the migration velocity model distributed with the data.

The model-based CDS stack is tailored to optimize the stacked section for a subsequent poststack depth migration. This is relevant for situations in which the generation of velocity models sufficiently accurate for prestack depth migration is difficult or even impossible. For the Sigsbee 2A data, we demonstrated that the model-based CDS stack allows to generate a poststack-migrated section very similar to the corresponding prestack migration result. The latter process usually requires a more accurate macro-velocity model.

The model-based CDS stack can be integrated into the CRS-based imaging workflow (see, e.g., Mann et al., 2003) in situations where the result of NIP wave tomography might not be sufficiently accurate to perform a prestack depth migration: as schematically shown in Figure 5, prestack migration might be replaced by a sequence of model-based CDS stack and poststack migration. In this way, we can overcome the former deficiencies of the CRS stack section which lead to gaps and artifacts in the poststack migration result.

References

- Höcht, G., de Bazelaire, E., Majer, P., and Hubral, P. (1999). Seismics and optics: hyperbolae and curvatures. *J. Appl. Geophys.*, 42(3,4):261–281.
- Jäger, R., Mann, J., Höcht, G., and Hubral, P. (2001). Common-Reflection-Surface stack: image and attributes. *Geophysics*, 66(1):97–109.
- Mann, J. (2001). Common-Reflection-Surface stack and conflicting dips. In *Extended abstracts, 63rd Conf. Eur. Assn. Geosci. Eng. Session P077*.
- Mann, J. (2002). *Extensions and applications of the Common-Reflection-Surface Stack method*. Logos Verlag, Berlin.
- Mann, J., Duvencak, E., Hertweck, T., and Jäger, C. (2003). A seismic reflection imaging workflow based on the Common-Reflection-Surface stack. *J. Seis. Expl.*, 12(3):283–295.
- Mann, J., Jäger, R., Müller, T., Höcht, G., and Hubral, P. (1999). Common-Reflection-Surface stack – a real data example. *J. Appl. Geophys.*, 42(3,4):301–318.
- Müller, T. (1998). Common Reflection Surface stack versus NMO/stack and NMO/DMO/stack. In *Extended abstracts, 60th Conf. Eur. Assn. Geosci. Eng. Session 1-20*.

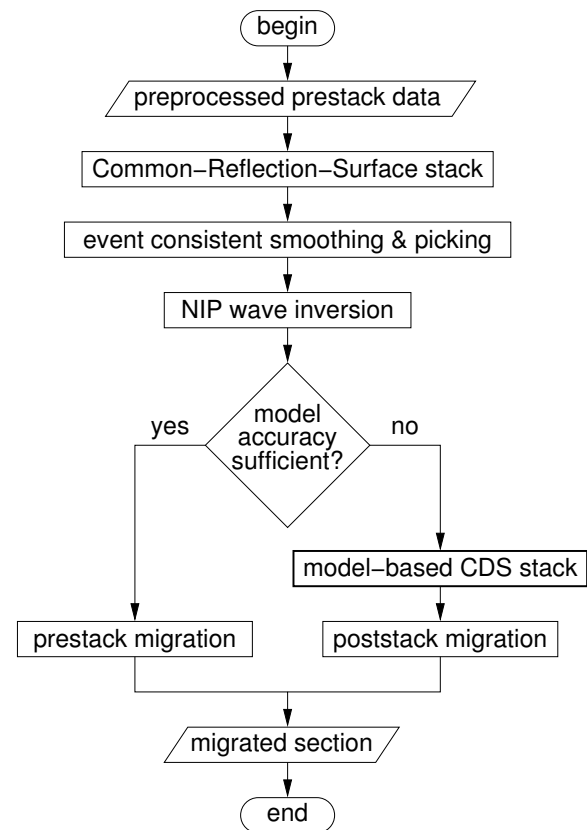


Figure 5: Processing flowchart with an alternative to prestack migration using the model-based CDS stack plus poststack depth migration.

- Pfaffenholz, J. (2001). Sigsbee2 synthetic subsalt data set: image quality as function of migration algorithm and velocity model error. In *Workshop on velocity model independent imaging for complex media, Extended abstracts*. Soc. Expl. Geophys. Session W5-5.
- Soleimani, M., Mann, J., Adibi Sedeh, E., and Piruz, I. (2010). Improving the seismic image quality in semi-complex structures in North East Iran by the CDS stack method. In *Extended abstracts, 72nd Conf. Eur. Assn. Geosci. Eng. Session P398*.
- Soleimani, M., Piruz, I., Mann, J., and Hubral, P. (2009a). Common-Reflection-Surface stack: accounting for conflicting dip situations by considering all possible dips. *J. Seis. Expl.*, 18(3):271–288.
- Soleimani, M., Piruz, I., Mann, J., and Hubral, P. (2009b). Solving the problem of conflicting dips in Common-Reflection-Surface stack. In *Extended Abstracts, 1st Internat. Conf. & Exhib., Shiraz, Iran*. Eur. Assn. Geosci. Eng.

Acknowledgments

This work was supported by the sponsors of the *Wave Inversion Technology (WIT) Consortium* and the *Ministry of Science, Research and Technology, Iran*. The Sigsbee 2A data have been provided by the *Subsalt Multiple Attenuation And Reduction Technology Joint Venture (SMAART JV)*.